Recent advances in optically isotropic liquid crystals for emerging display applications

Jin Yan, Meizi Jiao, Linghui Rao, and Shin-Tson Wu*

College of Optics and Photonics, University of Central Florida, Orlando, FL 32816, USA

ABSTRACT

Polymer-stabilized optically isotropic liquid crystal exhibits a fairly large Kerr constant and has potential to become next-wave display technology. The underlying physical mechanism is the Kerr-effect-induced isotropic-to-anisotropic transition. Wavelength and temperature effect on the Kerr constant of optically isotropic liquid crystal composites are investigated. Our experimental results indicate that as the wavelength or temperature increases, K decreases. The proposed physical models fit very well with the experimental data.

Keywords: Kerr constant, liquid crystal, optically isotropic

1. INTRODUCTION

Optically isotropic liquid crystal (LC) composites, which include polymer-stabilized blue phase (PSBP) and polymer-stabilized isotropic phase (PSIP), have been developed recently.[1-3] From macroscopic viewpoint, both PSBP and PSIP LC composites are optically isotropic in the voltage-off state due to self-assembled nanostructures. As the voltage increases, the induced birefringence gradually increases, which in turn causes phase retardation to the incident light. These LC composites exhibit some revolutionary features as compared to conventional nematic liquid crystals, such as isotropic dark state, submillisecond gray-to-gray response time[4], and no need for alignment layers. Therefore, they are quite attractive for fast response display and photonics applications. [5-9]

The underlying physical mechanism for the electric-field-induced isotropic-to-anisotropic transition is Kerr effect.[10] Kerr effect has been found in some liquids, such as benzene, CS_2, CCl_4, water, nitrotoluene, and nitrobenzene.[11-13] However, Kerr effect in liquid crystals has not been fully explored. Moreover, polymer-stabilized optically isotropic liquid crystal exhibits a fairly large Kerr constant (K), on the order of 1-10 nm/V^2, as compared to nitrobenzene, a well-known Kerr medium with $K\sim 2$ pm/V^2.[13] The large Kerr constant significantly lower the operating voltage.

In this paper, we first discuss the saturation behavior of Kerr effect in the high field region and then report the wavelength and temperature effects on the Kerr constant of a PSIP LC composite. Our experimental results show that Kerr constant decreases gradually as the wavelength or temperature increases. We fit the measured Kerr constant with physical models and good agreement is obtained between experiments and models. These results will undoubtedly help the optimization of PSIP LC devices by taking wavelength and temperature into considerations.

2. BRIEF REVIEW OF KERR EFFECT

When a Kerr medium, such as PSBP or PSIP LC composite, is subject to an electric field E, the induced birefringence is related to E as: [10]

$$\Delta n_{ind} = \lambda K E^2,\tag{1}$$

where λ is the wavelength and K the Kerr constant. From Eq. (1), the induced birefringence is linearly proportional to E^2, but this is valid only when the electric field is weak. As E keeps increasing, the induced birefringence will gradually saturate. The saturation phenomenon was observed in the high field region.[14, 15] To better describe the saturation trend of our experimental data, we proposed the following extended Kerr effect: [14]

$$\Delta n_{ind} = \Delta n_s (1 - \exp[-(E/E_s)^2]),\tag{2}$$

where Δn_s denotes the saturated induced birefringence and E_s the saturation electric field. In the weak field region ($E \ll E_s$), we can expand Eq. (2) using Taylor's expansion and deduce the Kerr constant as:

$$K \approx \Delta n_s / (\lambda E_s^2). \tag{3}$$

From Eq. (3), a BPLC material with high Δn_s and low E_s will result in a large Kerr constant. Roughly speaking, Δn_s governs the optical property (e.g., maximum phase change) while E_s determines the electric property (operating voltage) of a BPLC material. Kerr constant plays a key role on the operating voltage of the BPLC devices. A typical Kerr constant of BPLC composite is around 1 nm/V^2. In 2009, Kikcuhi et al.[16] reported a BPLC composite with K>10 nm/V^2 and its operating voltage in an in-plane-switching (IPS) cell (5 μm electrode width and 10 μm electrode gap) is ~50 V$_{rms}$. In addition to material, device configuration also plays a significant role for reducing the operating voltage. With protruded IPS electrodes, Rao et al.[7] showed that the operating voltage could be reduced to <10 V$_{rms}$. This is an important milestone as the BPLC device can then be addressed by amorphous silicon thin-film-transistors to achieve maximum transmittance.

3. WAVELENGTH EFFECT ON KERR CONSTANT

Figure 1 shows the experimental setup for measuring the electro-optic properties of a PSIP LC composite under different wavelengths. A narrow band interference color filter was placed in front of the white light source to select wavelength. In our experiment, five color filters with transmission peaks at λ~450 nm, 500 nm, 550 nm, 633 nm and 660 nm and bandwidth ~±5 nm were used and their corresponding voltage-dependent transmittance (VT) curves were measured. Since the white light source has an evident divergence angle, a group of lenses were used to collimate the light. In Fig. 1, we use one lens to represent this collimating lens group. A collimated light can travel a long distance without much divergence. Finally a focusing lens was used to collect the transmitted light into a photodiode detector.

The PSIP precursor used in this experiment was comprised of 56 wt% nematic LC host MLC-14200 (Merck), 29 wt% chiral dopants (24% CB15 and 5% ZLI-4572, Merck) and 15 wt% monomers (6% RM257 and 9% EHA) and a small amount (<1%) of photoinitiator. The LC/monomer mixture was injected to an in-plane switching (IPS) cell with electrode width ~10 μm, electrode gap ~10 μm, and cell gap ~7.5 μm. The cell was irradiated by UV light (λ~365 nm) at 70°C, which is well above the clearing temperature of the LC/monomer mixture. The LC cell was sandwiched between two crossed polarizers with the striped electrodes oriented at 45° with respect to the polarizer's transmission axis. We measured the VT curves at room temperature (~23°C) with different wavelengths.
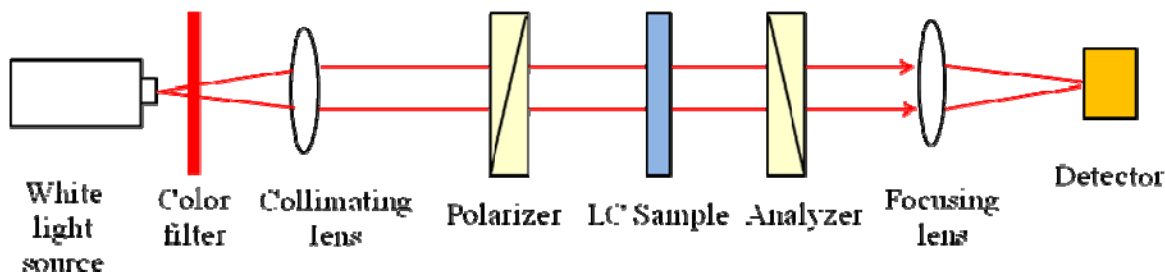

Fig. 1. Experimental setup for measuring the VT curves of a polymer-stabilized isotropic LC cell at different wavelengths.

Figure 2 shows the measured VT curves of the LC composite at five wavelengths. From left to right, the corresponding wavelengths are 450 nm, 500 nm, 550 nm, 633 nm and 660 nm. The transmittance at each wavelength is normalized to its own peak value. The operating voltage is lower at a shorter wavelength for two reasons: 1) phase retardation is inversely proportional to the wavelength, thus a shorter wavelength will exhibit a larger phase retardation under the same driving voltage; 2) birefringence decreases with wavelength under normal dispersion condition. Considering these two reasons, the required operating voltage is lower for a shorter wavelength.

To study the dispersion property of the PSIP LC composite, we carried out simulations to fit the experimental data shown in Fig. 2. First, the electric field distribution in our IPS cell was calculated at voltage-on states using finite element method.[17] Then at each wavelength we used the extended Kerr effect model [Eq. (2)] to calculate the induced

birefringence distribution according to the electric field distribution. Once the induced birefringence distribution was obtained, extended Jones Matrix method was employed to calculate the averaged transmittance.
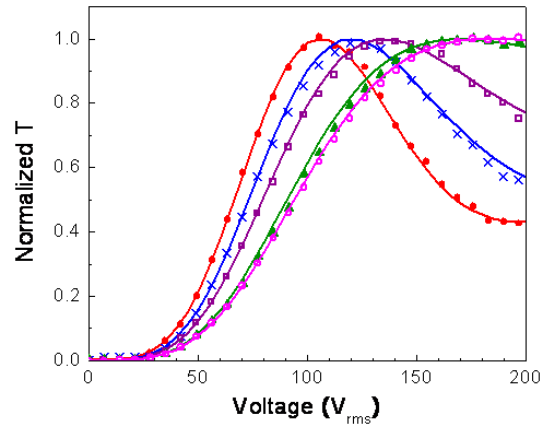

Fig. 2. Measured (dots) and fitted (lines) VT curves of the PSIP LC cell at different wavelengths. From left to right, the corresponding wavelengths are 450 nm, 500 nm, 550 nm, 633 nm and 660 nm.

The fitting results with Eq. (2) are shown in Fig. 2, in which dots represent experimental data and solid lines are fitting results. They overlap with each other very well at each wavelength. For each wavelength, there are two fitting parameters: Δn_s and E_s. The fitting results at each wavelength are listed in Table I.

Table I. Fitting results of the saturated birefringence (Δn_s), saturation electric field (E_s), and Kerr constant of the PSIP LC composite at the corresponding wavelength.

λ(nm)	Δn_s	E_s (V/μm)	K (m/V^2)
450	0.0730	6.8	3.51E-09
500	0.0695	6.8	3.01E-09
550	0.0670	6.8	2.63E-09
633	0.0635	6.8	2.17E-09
660	0.0630	6.8	2.06E-09

It is interesting to note that the fitting results of E_s keep the same for all the wavelengths studied. As abovementioned, Δn_s governs the optical property and E_s determines the electric property of a BPLC material. At a given temperature and voltage, the LC director reorientation profile is determined by the balance between elastic and electric torques. The LC director distribution will not be affected by the wavelength. Therefore, E_s does not vary with wavelength. However, the VT curves will be different for a different wavelength because the induced birefringence (Δn_{sat}) indeed depends on the wavelength, as shown in Table I. Moreover, the phase retardation varies with the wavelength.

As shown in Table I, the obtained Kerr constant decreases gradually with wavelength. Based on Eq. (3) and single-band birefringence dispersion model: [18.19]

$$\Delta n_s = G \frac{\lambda^2 \lambda^{*2}}{\lambda^2 - \lambda^{*2}} \tag{4}$$

where λ^* is the resonant wavelength of the LC composite and G is a proportionality constant, we derive the dispersion relation of Kerr constant as follows:

$$K = \frac{G\lambda\lambda^{*2}}{E_s^2(\lambda^2 - \lambda^{*2})} = \frac{A\lambda\lambda^{*2}}{\lambda^2 - \lambda^{*2}}$$

(5)

where $A = G/E_s^2$ is proportionality constant. For a conjugated LC compound, the two $\pi \rightarrow \pi*$ electronic transitions corresponding to λ^* usually occur in UV region [20]. In Fig. 3, we fitted the Kerr constant data with Eq. (5) using $\lambda^* \sim 216$ nm and $A \sim 0.0262$ nm^{-1}. The well-fitted data clearly demonstrate the implicit wavelength dependency of Kerr constant.
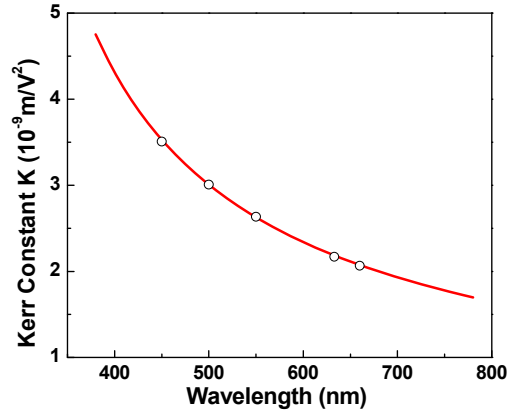

Fig. 3. Calculated Kerr constant at different wavelengths and the fitting results of the dispersion of Kerr constant of PSIP LC composites.

4. TEMPERATURE EFFECT ON KERR CONSTANT

In this experiment, the recipe of PSIP precursor is slightly different from the one used in the wavelength effect experiment. It consisted of 56.4% host nematic LC, 27.4% chiral dopants (22.7% CB15 and 4.7% ZLI-4572), 16.2% monomers (3.9% RM257, 4.6% Aldrich M1, and 7.7% EHA) and a small amount of photoinitiator. The reason that we mixed M1 is to try to lower the operating voltage.[21] The PSIP mixture was injected into an IPS cell with electrode width ~10 μm, electrode gap ~10 μm, and cell gap ~7.5 μm. UV curing process was performed at 70 °C (isotropic state) for 30 min. After polymerization, the clearing temperature of the BPLC composite was measured to be $T_c \sim 54$ °C, which was only ~5°C below that of the host LC/chiral mixture (before mixing with the monomers).

VT curves were measured by placing the IPS cell between two crossed polarizers. A CW He-Cd laser (λ=441.8 nm) was used as the light source. The main reason that we chose a shorter wavelength rather than a He-Ne laser (λ=633 nm) was to obtain transmission peak at a lower voltage. Figure 4 shows the normalized VT curves measured from 15°C to 37.5°C. As the temperature increases, the on-state voltage (V_{on}; corresponding to the peak transmittance) shifts to the right. With the same fitting method as described above, we fitted the VT curves shown in Fig. 1 with the extended Kerr effect model [Eq. (2)] at each temperature. The obtained K values are plotted in Fig. 5. Kerr constant decreases gradually as the temperature increases.

To explain this trend, we need to derive the temperature dependent Kerr constant. It has been reported by Gerber that the Kerr constant can be approximated by the following equation:[22]

$$K \sim \frac{\Delta n_{ind}}{\lambda E^2} \approx \Delta n \cdot \Delta\varepsilon \frac{\varepsilon_o P^2}{k\lambda(2\pi)^2}.$$

(6)

Here, Δn_{ind} is the induced birefringence, Δn, $\Delta\varepsilon$ and k are the intrinsic birefringence, dielectric anisotropy, and elastic constant of the host LC material, and P is the pitch length. Furthermore, we know that Δn, $\Delta\varepsilon$ and k are related to the nematic order parameter (S) as $\Delta n \sim \Delta n_o S$,[18] $\Delta\varepsilon \sim S/T$, and $k \sim S^2$.[23]
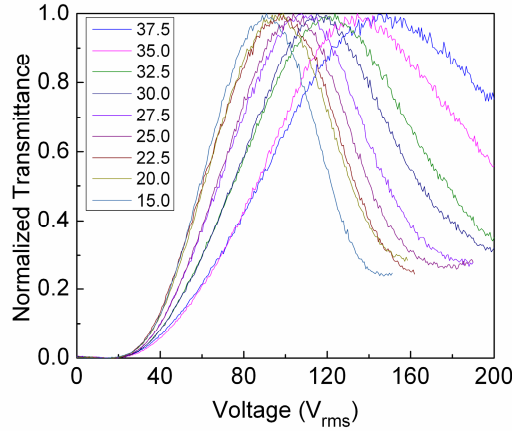
Fig. 4. Voltage dependent normalized transmittance curves of the PSIP LC composite measured from 15 $^{\circ}$C to 37.5 $^{\circ}$C. The IPS cell has electrode width=10 μm, electrode gap=10 μm, and cell gap=7.5 μm. λ=441.8 nm.
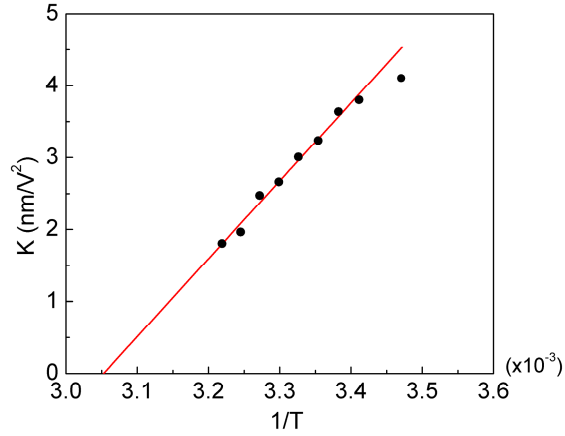

Fig. 5. Linear fitting of the Kerr constant with the reciprocal of temperature according to Eq. (8). T: Kelvin temperature. The fitting parameter is $\alpha = 1.08 \times 10^{-5}$ $m \cdot K/V^2$.

Plugging these parameters into Eq. (6) and ignoring the temperature effect of pitch length,[24,25] we find the temperature dependent Kerr constant has following simple form:

$$K \approx \Delta n \cdot \Delta \varepsilon \frac{\varepsilon_o P^2}{k \lambda (2\pi)^2} \sim \Delta n_o S \cdot \frac{S}{T} \cdot \frac{1}{S^2} \cdot \frac{\varepsilon_o P^2}{\lambda (2\pi)^2} \sim \alpha \cdot \frac{1}{T}. \tag{7}$$

From Eq. (7), Kerr constant is linearly proportional to the reciprocal temperature, and α is the proportionality constant. However, as the temperature approaches the clearing point (T_c) of the LC composite, Kerr constant should vanish (or at least dramatically decreased) because both Δn and $\Delta \varepsilon \to 0$. To satisfy this boundary condition, we rewrite Eq. (7) as follows:

$$K = \alpha \cdot \left(\frac{1}{T} - \frac{1}{T_c}\right). \tag{8}$$

Eq. (8) predicts that Kerr constant decreases linearly with reciprocal temperature ($1/T$) and eventually vanishes as the temperature reaches the clearing point of the LC composite.

To fit experimental data with Eq. (8), we treat the linear coefficient α and clearing temperature T_c as adjustable parameters. Results are depicted in Fig. 5. From fittings, we find $\alpha = 1.08 \times 10^{-5}$ m·K/V^2 and $T_c = 327.58$ K (54.43 ^{o}C). The obtained T_c matches very well with the measured clearing temperature (54 ^{o}C) of the LC composite. Thus, Eq. (8) actually has only one adjustable parameter which is α.

In Fig. 5, as the temperature decreases (or 1/T increases) the Kerr constant gradually deviates from the linear extrapolation. Although the reason is not yet completely clear, the Kerr constant in the low temperature region should not increase as rapidly as the fitting line shows. In the low temperature region, the higher order of order parameter should be taken into consideration.[26]

5. CONCLUSIONS

The wavelength and temperature effects on Kerr constant of polymer-stabilized optically isotropic LC composites are investigated. The experimental results indicate that the wavelength dependency of Kerr constant of PSIP composite can be described well by the single-band birefringence dispersion model, while the temperature dependency of Kerr constant follows the proposed analytical model very well. This information is particularly useful for display and photonic applications where both wavelength and temperature play important roles.

REFERENCES

[1] Kikuchi, H., Yokota, M., Hisakado, Y., Yang, H., and Kajiyama, T., "Polymer-stabilized liquid crystal blue phases," Nature Mater. 1, 64-68 (2002).

[2] Hisakado, Y., Kikuchi, H., Nagamura, T., and Kajiyama, T., "Large electro-optic Kerr effect in polymer-stabilized liquid-crystalline blue phases," Adv. Mater. 17, 96-98 (2005).

[3] Haseba, Y., Kikuchi, H., Nagamura, T., and Kajiyama, T., "Large electro-optic Kerr effect in nanostructured chiral liquid-crystal composites over a wide temperature range," Adv. Mater. 17, 2311-2315 (2005).

[4] Chen, K. M., Gauza, S., Xianyu, H., and Wu, S. T., "Submillisecond gray-level response time of a polymer-stabilized blue phase liquid crystal," J. Disp. Technol. 6, 49-51 (2010).

[5] Ge, Z., Gauza, S., Jiao, M., Xianyu, H. and Wu, S. T., "Electro-optics of polymer-stabilized blue phase liquid crystal displays," Appl. Phys. Lett. 94, 101104 (2009).

[6] Ge, Z., Rao, L., Gauza, S., and Wu, S. T., "Modeling of blue phase liquid crystal displays," J. Disp. Technol. 5, 250-256 (2009).

[7] Rao, L., Ge, Z., Wu, S. T., and Lee, S. H., "Low voltage blue-phase liquid crystal displays," Appl. Phys. Lett. 95, 231101 (2009).

[8] Jiao, M., Li, Y. and Wu, S. T., "Low voltage and high transmittance blue-phase liquid crystal displays with corrugated electrodes," Appl. Phys. Lett. 96, 011102 (2010).

[9] Yoon, S., Kim, M., Kim, M. S., Kanga, B. G., Kim, M. K., Srivastavaa, A. K., Lee, S. H., Ge, Z., Rao, L., Gauza, S., and Wu, S. T., Liq. Cryst. 37, 201 (2010).

[10] Kerr, J., "A New Relation between Electricity and Light: Dielectrified Media Birefringent," Philos. Mag. 50, 337-348 (1875).

[11] Yariv, A. and Yeh, P., [Optical Waves in Crystal], Wiley, New York, (2002).

[12] Beams, J. W., "Electric and magnetic double refraction," Rev, Mod. Phys. 4, 133-172 (1932).

[13] McComb, H. E., "Dispersion of electric double refraction and ordinary dispersion in liquids," Phys. Rev. 29, 525-540 (1909).

[14] Yan, J., Cheng, H. C., Gauza, S., Li, Y., Jiao, M., Rao, L. and Wu, S. T., "Extended Kerr effect of polymer-stabilized blue-phase liquid crystals," Appl. Phys. Lett. 96, 071105 (2010).

[15] Yan, J., Jiao, M., Rao, L., and Wu, S. T., "Direct measurement of electric-field-induced birefringence in a polymer-stabilized blue-phase liquid crystal composite," Opt. Express 18, 11450-11455 (2010).

[16] Kikuchi, H., Haseba, Y., Yamamoto, S., Iwata, T. and Higuchi, H., "Optically Isotropic Nano-structured Liquid Crystal Composites for Display Applications," SID Symposium Digest 40, 578-581 (2009).

[17] Jin, J., [The Finite Element Method in Electromagnetics (2nd edition)], Wiley-IEEE Press, NJ, (2002)

[18] Wu, S. T., "Birefringence dispersion of liquid crystals," Phys. Rev. A 33, 1270-1274 (1986).

[19] Wu, S. T., Wu, C. S., Warenghem, M., and Ismaili, M., "Refractive index dispersions of liquid crystals," Opt. Eng. (Bellingham) 32, 1775-1780 (1993).

[20] Wu, S. T., Ramos, E., and Finkenzeller, U., "Polarized UV spectroscopy of conjugated liquid crystals" J. Appl. Phys. 68, 78-85 (1990).

[21] Fan, Y. H., Lin, Y. H., Ren, H., Gauza, S. and Wu, S. T., "Fast-response and scattering-free polymer network liquid crystals," Appl. Phys. Lett. 84, 1233 (2004).

[22] Gerber, P. R., "Electro-optical effects of a small-pitch blue-phase system," Mol. Cryst. Liq. Cryst. 116, 197 (1985).

[23] Maier, W., and Saupe, A., "A simple molecular-statistical theory for nematic liquid crystal phase, part II," Z. Naturforsch, Teil A 15, 287 (1960).

[24] Zhang, F. and Yang, D. K., "Temperature-dependence of pitch and twist elastic constant in cholesteric to smectic A phase transition," Liq. Cryst. 29, 1497 (2002).

[25] Rao, L., Yan, J. and Wu, S. T., "Prospects of emerging polymer-stabilized blue-phase liquid crystal displays," J. Soc. Info. Display 18, 954-959 (2010).

[26] Rao, L., Gauza, S. and Wu, S. T., "Low temperature effects on the response time of liquid crystal displays," Appl. Phys. Lett. 94, 071112 (2009).